

A Shallow Water Model for Computing Inland Inundation due to Indonesian Tsunami 2004 using a Moving Coastal Boundary

Md. Fazlul Karim, Mohammed Ashaque Meah, and Ahmad Izani M. Ismail

Abstract—In this paper, a two-dimensional mathematical model is developed for estimating the extent of inland inundation due to Indonesian tsunami of 2004 along the coastal belts of Peninsular Malaysia and Thailand. The model consists of the shallow water equations together with open and coastal boundary conditions. In order to route the water wave towards the land, the coastal boundary is treated as a time dependent moving boundary. For computation of tsunami inundation, the initial tsunami wave is generated in the deep ocean with the strength of the Indonesian tsunami of 2004. Several numerical experiments are carried out by changing the slope of the beach to examine the extent of inundation with slope. The simulated inundation is found to decrease with the increase of the slope of the orography. Correlation between inundation / recession and run-up are found to be directly proportional to each other.

Keywords—Inland Inundation, Shallow Water Equations, Tsunami, Moving Coastal Boundary.

I. INTRODUCTION

LARGE population and public property are usually concentrated in the coastal areas and its protection from natural hazards such as tsunami and storm surges is very important. The Indonesian tsunami of 2004 is vivid evidence that the design codes of coastal infrastructure, in the inundation zone, need to take into account this extreme event. Inundation associated with extreme sea levels is the main factor which leads to the loss of life and property whenever a tsunami hits the coast. Loss of life may be minimized if extreme sea levels and the associated coastal inundation is predicted well in advance. Such a risk assessment requires the use of mathematical models to simulate the generation, the propagation across the ocean, and eventually, the overland run-up of a tsunami.

Numerical simulations of the extent of inundation due to long waves such as tsunami have been carried out by many researchers [4], [6], [19], [12], [14], [15]. Lynch and Gray [9] developed a technique for the simulation of shallow water flow which deforms continuously in time and used a moving

grid in their solution procedure. Cho et al. [4] developed a coupled numerical model based on the shallow-water equations to simulate the 1983 Nihonkai-Chubu Earthquake tsunami across the East Sea. Viana-Baptista et al. [14] did the flood calculation along Tagus Estuary of Lisbon coastal area. Wijetunge [15] estimated the extent of inundation in Sri Lanka due to the Indonesian tsunami 2004 based on damage to structures, lines of debris and location of wreckage as well as eyewitness accounts of overland flow. Inan and Blas [6] developed a numerical model for the simulation of long wave propagation and run-up accounting for the bottom friction. They used a moving boundary and a staggered grid to overcome the difficulty of determining wet and dry points in their computations and take the total depth as a positive value at a wet point and zero on the boundary. Roy et al. [12] developed a one-dimensional mathematical model for estimating the extent of inland inundation along a coastal belt due to long waves originating through astronomical tide and tsunami. They examined the extent of inundation with respect to different slopes along the beach.

The Indian coast including Peninsular Malaysia and Thailand was affected five times due to tsunamis during the last 125 years (1883 – 2007), while the frequency of tsunamis in the Pacific Ocean is five per year. Maybe due to their lesser frequency, not much attention has been paid to tsunamis in this region. Devastating tsunamis occur periodically around the world, although none captured people's attention as vividly as the magnitude - 9.0 earthquake which occurred offshore of Banda Aceh, Indonesia on December 26, 2004.

In this study, a numerical model is developed for estimating the extent of inundation along the coastal belt of Peninsular Malaysia and Thailand due to 26 December 2004 Indian Ocean tsunami. The model domain is a region between 2° N to 14° N and 91° E to 100.5° E that include both west coast of Peninsular Malaysia and Thailand as well as the tsunami source region along Sumatra-Andaman fault line (Fig. 1). In this study, a boundary fitted curvilinear grid system similar to Karim et al. [7] is developed to compute the extent of inundation along the west coast of Peninsular Malaysia and southern Thailand. The west coasts of Malaysia, Southern Thailand and the western open sea boundary are represented by two functions. On the other hand, the north and south open sea boundaries were considered as straight lines. The coastal boundary of the model domain is considered as moving with respect to time to allow the flow of sea water across the initial

M.F. Karim is with the Institute Technology Brunei, Brunei (phone: +673 7157167; e-mail: mdfazlulkk@yahoo.com).

M. A. Meah is with the Shahjalal University of Science and Technology, Bangladesh Institute Technology Brunei, Brunei (e-mail: mamsust@yahoo.com).

A.I.M. Ismail is with the Universiti Sains Malaysia, Malaysia (e-mail: izani@cs.usm.my).

position of the coastline towards the land. A special technique is used to monitor the continuous movement of the coastline with respect to its initial position. Comparison of maximum run-up along the coast obtained from the model of moving boundary and the model of fixed coastal boundary is carried out. A correlation between inundation and run-up is also established.



Fig. 1 Model domain including west coast of Thailand, Peninsular Malaysia and source zone west of north Sumatra (Source: Karim et al. 2007)

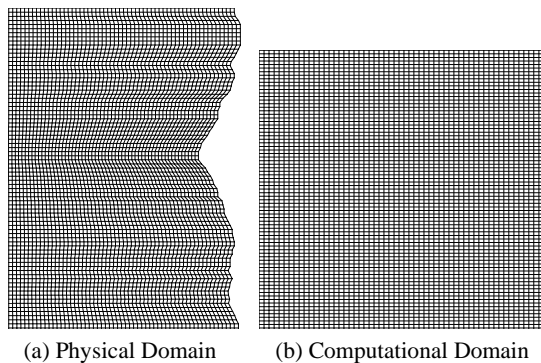


Fig. 2 Boundaries and grid system; (a) curvilinear boundaries and the curvilinear grid system, (b) rectangular boundaries and the rectangular grid system

II. BOUNDARY-FITTED GRIDS

A system of rectangular Cartesian coordinates is used in which the origin O , is within the equilibrium of the sea-surface. Ox points towards the west, Oy points towards the north and Oz is directed vertically upwards. The displaced position of the sea-surface is given by $z = \zeta(x, y, t)$ and the position of the sea-floor is given by $z = -h(x, y)$. The eastern moving coastal boundary is situated at $x = b_1(y, t)$ with the initial position at $x = b_1(y, 0)$ and the western open-sea boundary is at $x = b_2(y)$. The southern and the northern open-sea boundaries are at $y = 0$ and $y = L$ respectively. This configuration is shown in Fig. 2. The western, southern and northern open sea boundaries are considered as fixed.

The system of gridlines oriented to $x = b_1(y, t)$ and $x = b_2(y)$ are given by the generalized function

$$x = \{(m-l)b_1(y, t) + lb_2(y)\} / m \quad (1)$$

where m is the number of gridlines in x -direction and l is an integer such that $0 \leq l \leq m$.

The system of gridlines oriented to $y = 0$ and $y = L$ are given by the generalized function

$$y = \{(n-p)0 + pL\} / n \quad (2)$$

where n is the number of gridlines in y -direction and p is an integer such that $0 \leq p \leq n$.

The equation (1) reduces to $x = b_1(y, t)$ and $x = b_2(y)$ for $l = 0$ and $l = m$ respectively. Similarly equation (2) reduces to $y = 0$ and $y = L$ for $p = 0$ and $p = n$ respectively. Now by proper choice of l, m and p, n the boundary-fitted curvilinear grids can be generated.

III. MATHEMATICAL FORMULATION

A. The Shallow Water Equations

$$\frac{\partial \zeta}{\partial t} + \frac{\partial \tilde{u}}{\partial x} + \frac{\partial \tilde{v}}{\partial y} = 0 \quad (3)$$

$$\frac{\partial \tilde{u}}{\partial t} + \frac{\partial (u\tilde{u})}{\partial x} + \frac{\partial (v\tilde{u})}{\partial y} - f\tilde{v} = -g(\zeta+h)\frac{\partial \zeta}{\partial x} - \frac{C_f \tilde{u}(u^2+v^2)^{1/2}}{\zeta+h} \quad (4)$$

$$\frac{\partial \tilde{v}}{\partial t} + \frac{\partial (u\tilde{v})}{\partial x} + \frac{\partial (v\tilde{v})}{\partial y} + f\tilde{u} = -g(\zeta+h)\frac{\partial \zeta}{\partial y} - \frac{C_f \tilde{v}(u^2+v^2)^{1/2}}{\zeta+h} \quad (5)$$

where, $(\tilde{u}, \tilde{v}) = (\zeta + h)(u, v)$

Here u and v are the x and y components of velocity of sea water respectively, g is gravity, f is the Coriolis parameter, ζ is the displacement of the free surface from the equilibrium state, C_f is the bottom friction coefficient, h is the ocean depth from mean sea level.

B. The Boundary Conditions

The coastal boundary may be of two types: the coastline consists of a vertical side wall or the shoreline moves with the same velocity as that of the approaching water. Following

Dube et al. [5], in case of fixed coastal boundary the condition is:

$$u - v \frac{\partial b_1}{\partial y} = 0 \text{ along } x = b_1(y, 0) \quad (6)$$

and, in case of moving coastal boundary the condition is:

$$u - \frac{\partial b_1}{\partial t} - v \frac{\partial b_1}{\partial y} = 0 \text{ along } x = b_1(y, t) \quad (7)$$

Following Karim et al. [8], boundary conditions along the open boundaries are:

$$v + (g/h)^{1/2} \zeta = 0 \text{ along } y = 0 \quad (8)$$

$$v - (g/h)^{1/2} \zeta = 0 \text{ along } y = L \quad (9)$$

$$u - v \frac{\partial b_2}{\partial y} - (g/h)^{1/2} \zeta = 0 \text{ along } x = b_2(y) \quad (10)$$

C. Coordinate Transformation

To facilitate the numerical treatment of the bending coastal boundary, according to Dube et al. [5], the following coordinate transformation is introduced:

$$\eta = \frac{x - b_1(y, t)}{b(y, t)} \text{ where } b(y, t) = b_2(y) - b_1(y, t) \quad (11)$$

Accordingly, the equations (1)-(10) will be transformed to new set of equations in the η - y domain. A detailed similar (not same) description of Coordinate transformation, representations of Islands and transformed shallow water equations and boundary conditions are available in Karim et al. [7].

In case of inland intrusion of water, the continuously deforming position of the coastline is ensured by kinematical boundary condition (7). A further requirement is that the depth of water be zero at the coastline. Thus following Dube et al. [5], at $x = b_1(y, t)$ or $\eta = 0$

$$\zeta(\eta = 0, y, t) + h(x = b_1(y, t), y) = 0 \quad (12)$$

Depending on whether $b_1(y, t) > b_1(y, 0)$ or $b_1(y, t) < b_1(y, 0)$, interpolation or use new inland orographical data is used to fix the value of $h(x = b_1(y, t), y)$. This may be achieved by differentiating Eq. (12) with respect to t to yield:

$$\frac{\partial \zeta}{\partial t}(\eta = 0, y, t) + S \frac{\partial b_1}{\partial t} = 0 \quad (13)$$

Where

$$S = \left[\frac{\partial h}{\partial x} \right]_{x=b_1(y, t)} \quad (14)$$

Equation (13) gives the value of $b_1(y, t)$ at any time t . For a constant value of S , by integrating Eq. (13) we get,

$$b_1(y, t) = b_1(y, 0) - \frac{1}{S} \zeta(\eta = 0, y, t) \quad (15)$$

From Eq. (15), it is evident that, if $\zeta(\eta = 0, y, t) < 0$, the water surface at the coastline is depressed and so the coastline will recede from its initial position. If $\zeta(\eta = 0, y, t) > 0$, water surface at the coastline rises above its equilibrium level and so there is corresponding inland intrusion of water. The inland intrusion of water may be determined by:

$$\mu(y, t) = b_1(y, t) - b_1(y, 0) \quad (16)$$

IV. NUMERICAL DISCRETISATION

The transformed shallow water equations and boundary conditions are solved by the finite difference method using a staggered (χ, λ) grid.

We define the grid points (η_i, λ_j) in the domain by

$$\chi_i = (i - 1) \Delta \chi, \quad i = 1, 2, 3, \dots, m \quad (17)$$

$$\lambda_j = (j - 1) \Delta \lambda, \quad j = 1, 2, 3, \dots, n \quad (18)$$

The sequence of discrete time instants is given by

$$t_k = k \Delta t, \quad k = 1, 2, 3, \dots$$

The curvilinear and the corresponding rectangular boundaries and grids are shown in Fig. 2. The χ -axis is directed towards west at an angle 15° (anticlockwise) with the latitude line and the λ -axis is directed towards north inclined at an angle 15° (anticlockwise) with the longitude line. The number of grids in χ and λ -directions are respectively $m = 230$ and $n = 319$ and the grid size is chosen to be equal to 4 km. The model area includes the source region of Indonesian tsunami 2004. The time step of computation is determined to satisfy the stability condition (Courant condition). It is set to 10 s in this computation. Following Kowalik et al. [8], the value of the friction coefficient C_f is taken as 0.0033 throughout the model area. The depth data for the model area are collected from the Admiralty bathymetric charts.

V. INITIAL CONDITION (TSUNAMI SOURCE GENERATION)

The generation of an earthquake tsunami source depends essentially on the pattern and dynamics of motions in the earthquake source zone and on the initial seafloor movements. The generation mechanism of the 2004 Indonesian tsunami was mainly a static sea floor uplift caused by an abrupt slip at the India/Burma plate interface. A detailed description of the estimation of the extent of the earthquake rupture as well as the maximum uplift and subsidence of the seabed is given in Kowalik et al. [8] and this estimation is based on Okada [10]. From the deformation contour, it is seen that the estimated uplift and subsidence zone is between 92° E to 97° E and 2° N

to 10°N with a maximum uplift of 507 cm at the west and maximum subsidence of 474 cm at the east (Fig. 4 of Kowalik et al. [8]). The uplift to subsidence is approximately from west to east relative to the west coasts of the Malaysian Peninsula and Thailand. The major force of tsunamis is the vertical displacement of the seafloor. For computational purposes tsunami models are often initialized by a sea-surface displacement. We can assume that the initial value of the sea surface displacement that starts a tsunami is the same as the vertical displacement of the sea floor (Arreaga-Vargas et al., [1]; Aida, [3], due to incompressibility of the ocean water. Following Kowalik et al. [8], the disturbance in the form of rise and fall of sea surface is assigned as the initial condition in both the models with a maximum rise of 5 m to maximum fall of 4.75 m. Ammon et al. [2] reported the rupture zone between 92° E to 97°E and 2°N to 13°N. Tanioka et al. [14] estimated the rupture zone between 92° E to 97°E and 2°N to 13.5°N. Based on the above information we consider the source, extended along the fault line between 92° E to 97°E and 2°N to 10°N for our model. In all other regions the initial sea surface elevations are taken as zero. Also the initial x and y components of velocity are taken as zero throughout the model area.

VI. RESULT AND DISCUSSION

The extent of inundation along the western coastal belt of Peninsular Malaysia and Thailand is presented. A correlation between inundation and water level is established. A comparison of maximum water level along the coast obtained from the model of moving boundary and the model of fixed coastal boundary is also carried out.

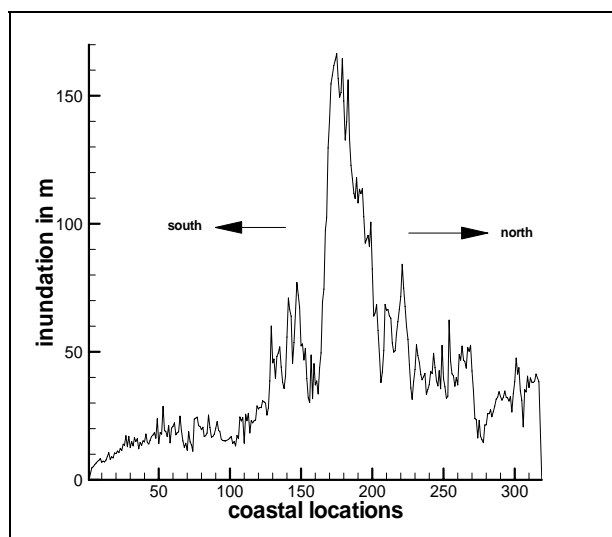


Fig. 3 Maximum inland inundation along the west coast of Peninsular Malaysia and Thailand for 8 degree inclination

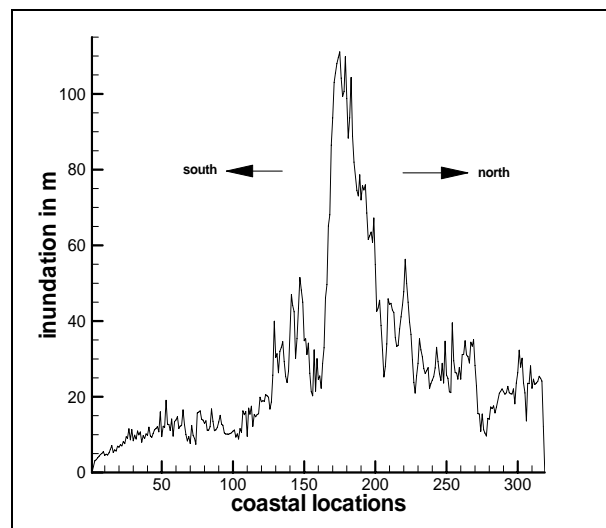


Fig. 4 Maximum inland inundation along the west coast of Peninsular Malaysia and Thailand for 12 degree inclination

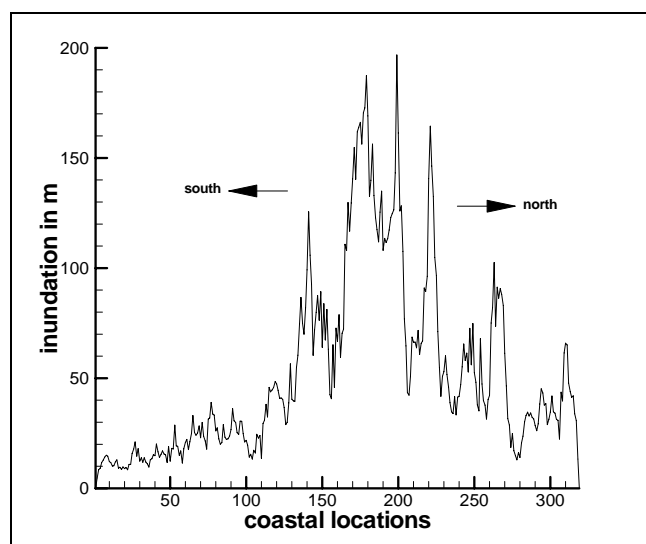


Fig. 5 Maximum inland inundation along the west coast of Peninsular Malaysia and Thailand for variable inclination

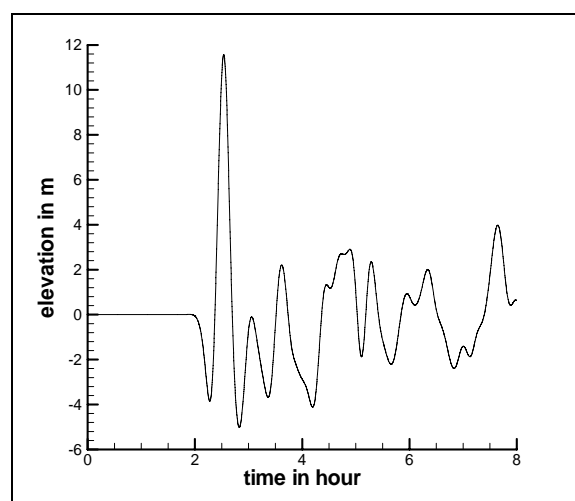


Fig. 6 Computed tsunami response along the coast

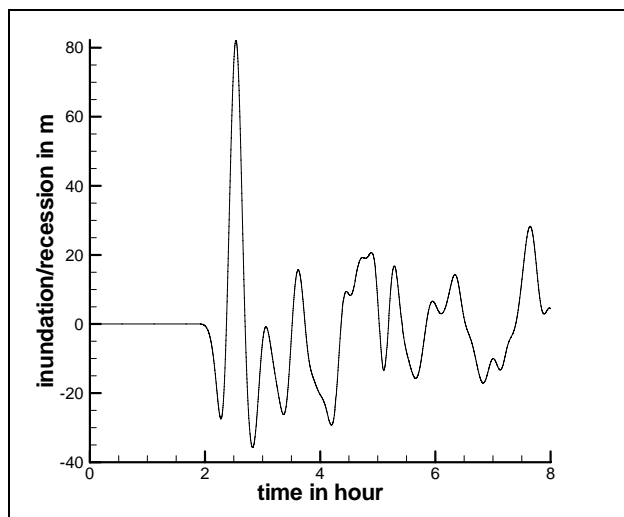


Fig. 7 Computed inundation/recession along the coast due to 8 degree inclination

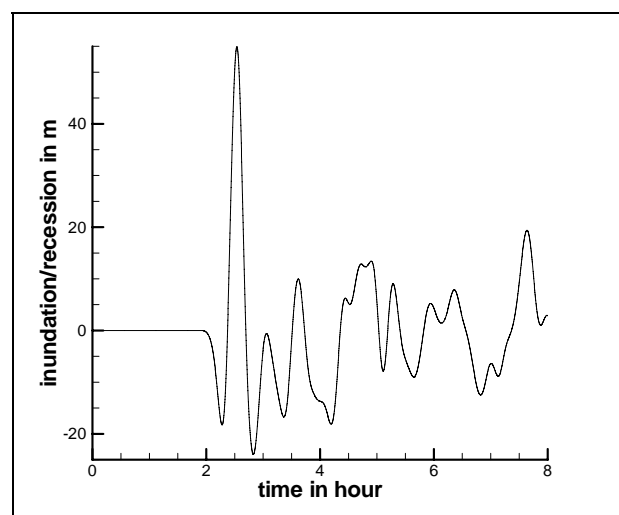


Fig. 8 Computed inundation/recession along the coast due to 12 degree inclination

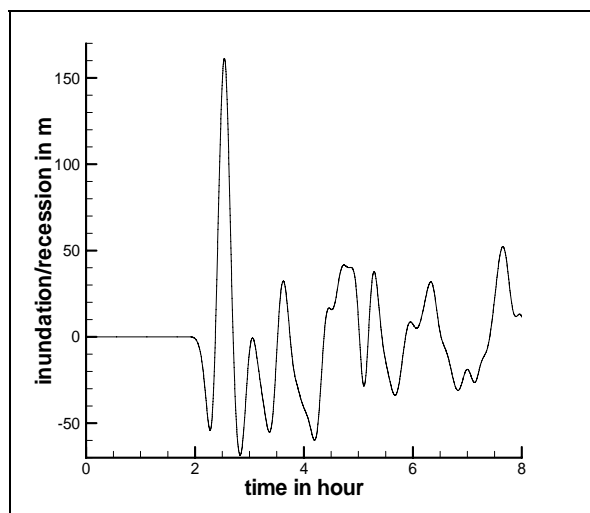


Fig. 9 Computed inundation/recession along the coast due to inclination of variable degree

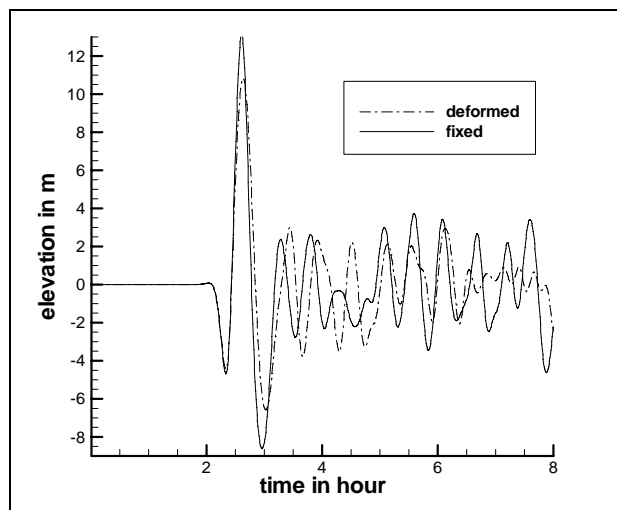


Fig. 10 Computed water levels along a particular position of the coast due to fixed boundary and deformed/moving coastal boundary

A. Extent of Inundation

Fig. 3 depicts the maximum inland inundation along the west coast of Thailand and Peninsular Malaysia for an inclination of 8 degrees. The maximum inland intrusion along west coast of Peninsular Malaysia is ~30 m while along Thailand it is ~170 m. As the on-shore slope increases from 8 degree to 12 degree the extent of inundation decreases to ~20 m and ~115 m for Malaysian and Thailand coast respectively (Fig. 4). If the slope is not constant and varies from 8 degree to 12 degree the inundation is ~40 m and ~200 m respectively (Fig. 5). So the tsunami inundation is controlled by the configuration of the beach. Papadopoulos et al. [11] conducted a post tsunami field survey along the coastal belt of southern Thailand. According to the eyewitnesses reported that the tsunami inundation in the Patong beach of Thailand varied from 150 m to at least 750 m. One eyewitness reported inundation of only 20 m. In Maya Bay, eyewitnesses reported that the tsunami wave inundated for about 200 to 300 meters. But we failed to get any information regarding on the extent of inundation along Malaysian coast. Moreover, the actual on-shore slope of the coastal belt is not considered in the model computations. However our computed result shows good agreement with the field survey report of Papadopoulos et al. [12].

B. Correlation between Inundation and Water Level

Fig. 6 shows the computed time series of water level at a coastal location of Thailand about 140 km north of Phuket due to the initial tsunami generated at Sumatra on 26 December 2004. The tsunami response begins with recession that reaches up to minimum level of -3.8 m before rising up; then the water level gradually increases to reach a maximum level of 11.6 m. The water level then oscillates continuously for several hours with low amplitude. Fig. 7 shows the inundation and recession for the same coastal location associated with the tsunami wave as shown in Fig. 6. For 8 degree inclination the inland inundation/recession curve is consistent with the water

REFERENCES

- [1] Aida, I., "Numerical Computation of a Tsunami Based on a Fault Origin Model of an Earthquake", *J. Seismol. Soc. Japan*, 27, 141-154, 1974.
- [2] Ammon, C. J., Ji, C., Thio, H.-K., Robinson, D., Ni, S., Hjorleifsdottir, V., Kanamori, H., Lay, T., Das, S., Helmberger, D., Ichinose, G., Polet, J. & Wald, D., "Rupture Process of the 2004 Sumatra-Andaman Earthquake", *Science*, 308(5725), 1133 – 1139, 2005.
- [3] Arreaga-Vargas, P., Ortiz, M. & Farreras, S.F., "Mapping the Possible Tsunami Hazard as the First Step Towards a Tsunami Resistant Community in Esmeraldas, Ecuador. In K. Satake (Ed.), *Tsunamis: Case Studies and Recent Developments* (pp. 203 - 215). Netherlands: Springer, 2005.
- [4] Cho, Y.-S., Jin, S.-B., & Lee, H.-J., "Safety analysis of Ulchin Nuclear Power Plant against Nihonkai-Chubu Earthquake Tsunami", *Nuclear Engineering and Design*, 228(1-3), 393-400, 2004.
- [5] Dube, S. K., Sinha, P.C., & Roy, G.D. , "The Effect of a Continuously Deforming Coastline on the Numerical Simulation of Storm Surge in Bangladesh", *Mathematics and Computers in Simulation*, 28, 41 – 56, 1986.
- [6] Inan, A., & Balas, L. A., "Moving Boundary Wave Run-Up Model. In Y. Shi, Albada, G.D.v., Dongarra", J., & Sloot, P.M.A. (Ed.), *Computational Science – ICCS* (pp. 38-45). Berlin / Heidelberg: Springer, 2007.
- [7] Karim, M. F., Roy, G.D., Ismail, A.I.M., & Meah, M.A. , "A Shallow Water Model for Computing Tsunami along the West Coast of Peninsular Malaysia and Thailand Using Boundary-Fitted Curvilinear Grids" *Science of Tsunami Hazards*, 26(1), 21 – 41, 2007.
- [8] Kowalik, Z., Knight, W., & Whitmore, P. M., "Numerical Modeling of the Tsunami: Indonesian Tsunami of 26 December 2004", *Sc. Tsunami Hazards*, 23(1), 40 – 56, 2005.
- [9] Lynch, F. R., & Gray, W.G., "Finite Element Simulation of Flow in Deforming Regions, 1980. *J. Comput. Phys.*, 36, 135 – 153, 1980.
- [10] Okada, Y., "Surface Deformation due to Shear and Tensile Faults in a Half Space", *Bull. Seism. Soc. Am.*, 75, 1135 – 1154, 1985.
- [11] Papadopoulos, G. A., Caputo, R., McAdoo, B., Pavlides, S., Karastathis, V., Fokaefs, A., Orfanogiannaki, K. & Valkaniotis, S., "The large tsunami of 26 December 2004: Field observations and eyewitness accounts from Sri Lanka, Maldives Is. and Thailand", *Earth Planets Space*, 58, 233 – 241, 2006.
- [12] Roy, G. D., Karim, M. F., & Ismail, A. M., "A 1-D Shallow Water Model for Computing Inland Inundation due to Long Waves Using a Moving Boundary", *Far East J. Appl. Math.*, 28(3), 395 – 408, 2007.
- [13] Tanioka, Y., Yudhicara, Kususose, T., Kathirolu, S., Nishimura, Y., Iwasaki, S. & Satake, K. "Rapture process of 2004 great Sumatra-Andaman earthquake estimated from tsunami waveforms," *Earth Planets Space*, 58, 203 – 209, 2006.
- [14] Viana-Baptista, M. A., Soares, P.M., Miranda, J.M. & Luis, J.F., "Tsunami Propagation along Tagus Estuary (Lisbon, Portugal) Preliminary Results", *Science of Tsunami Hazards*, 24(5), 329 – 338, 2006.
- [15] Wijetunge, J. J., "Tsunami on 26 December 2004: Spatial distribution of tsunami height and the extent of inundation in Sri-Lanka, *Science of Tsunami Hazard*, 24(3) 225-239, 2006.

level fluctuation (Fig. 6) with a maximum inundation of ~82 m and maximum recession of ~35 m (Fig. 7). Since the constant slope is considered, the curve of inundation/recession should be consistent with that of sea surface fluctuation as shown in Fig. 6. As the on-shore slope increases the computed inundation/recession remains qualitatively the same but both inundation and recession amplitudes gradually decrease. The maximum inundation and recession for 12 degree inclination are ~55 m and ~24 m respectively (Fig. 8). For a variable (from 8 to 12) degree inclination the inundation and recession are ~165 m and ~65 m respectively (Fig. 9). Thus the inundation/recession and water level seem to be directly proportional to each other.

C. Comparison between the Maximum Water Levels due to Moving Boundary and Fixed Coastal Boundary

Fig. 10 shows the time series of water levels at a particular coastal location near the south of Phuket Island, Thailand due to moving and fixed coastal boundary. It may be seen that the maximum water levels due to moving boundary is ~10.75 m. On the other hand, the peak surge is ~13 m due to fixed coastal boundary. The surge height due to fixed boundary is considerably higher than that of the moving boundary. This may be due to the unrealistic piling up of water at the vertical side wall boundary. With a moving boundary, this piling up does not occur since the water is allowed to flow freely inland thus reducing the maximum sea surface elevation at the initial position of the coast line and causing the inundation. The comparison for other coastal locations (not shown in the figure) indicates that there is no significant difference in the maximum sea surface elevations along the coast. Dube et al. [5] simulated the 1970 Chittagong cyclone and associated coastal inundation in Bangladesh. They observed a significant difference in peak surge at Majidi along Bangladesh coast due to fixed coastal boundary and moving boundary but no significant difference in the peak surge along rest of the coast line. So our comparison is consistent with that of Dube et al. [5].

VII. CONCLUSION

A two dimensional tsunami inundation model based on the shallow-water theory has been developed for simulating the extent of inundation along the western coast of Peninsular Malaysia and southern Thailand due to the 24 December 2004 Indonesian tsunami. The inundation along the coastal belt of the west coast of Peninsular Malaysia and southern Thailand is found to decrease with the increase of the slope of the beach and the inundation is controlled by the configuration of the beach. An investigation was carried out to test the relation between the maximum water level and inundation/recession along the coast and it seems that the inundation/recession and water level are directly proportional to each other. A comparison of maximum water levels due to moving boundary and fixed coastal boundary was also carried out. The water elevation due to fixed boundary is considerably higher than that of moving boundary. The proposed numerical model successfully simulates the long wave inundation along the coast.